General Disclaimer

One or more of the Following Statements may affect this Document

- This document has been reproduced from the best copy furnished by the organizational source. It is being released in the interest of making available as much information as possible.

- This document may contain data, which exceeds the sheet parameters. It was furnished in this condition by the organizational source and is the best copy available.

- This document may contain tone-on-tone or color graphs, charts and/or pictures, which have been reproduced in black and white.

- This document is paginated as submitted by the original source.

- Portions of this document are not fully legible due to the historical nature of some of the material. However, it is the best reproduction available from the original submission.

NASA TECHNICAL MEMORANDUM

NASA TM X-71807

NASA TM X-71807

ACOUSTICS OF ATTACHED AND PARTIALLY ATTACHED FLOW FOR
SIMPLIFIED OTW CONFIGURATIONS WITH 5:1 SLOT NOZZLE

by U. von Glahn and D. Groesbeck
Lewis Research Center
Cleveland, Ohio 44135

OCT 1975
RECEIVED
NASA STI FACILITY
INPUT BRANCH

ACOUSTICS OF ATTACHED AND PARTIALLY ATTACHED FLOW FOR

SIMPLIFIED OTW CONFIGURATIONS WITH 5:1 SLOT NOZZLE

by U. von Glahn and D. Groesbeck
Lewis Research Center

ABSTRACT

The acoustics of simple engine over-the-wing configurations, with complete and partially attached jet flow to the shielding surface were studied at model scale. The nozzle used consisted of a 5:1 slot nozzle (equivalent diameter, 5.1 cm) operated at a nominal jet Mach number of 0.6, with the flow directed parallel to and at angles up to 10° toward the shielding surface (flat board). The shielding length of the surface was varied from 15 to 54.4 cm, and the nozzle height above the surface was varied from 0 to 4.45 cm. The flow field at the trailing edge of each nozzle/surface configuration was mapped. The aerodynamic results indicate that, with attached flow, the jet flow field is stretched in the flow direction resulting in locally higher velocities than those for partially attached flow or nozzle only flow. The stretching of the flow field increased the noise levels for the attached flow cases compared to those with only partially attached flow. With attached flow, the shielding benefits were substantially reduced compared with fully detached flow. Increasing the impingement angle of the jet flow from 0° to 10° generally caused the noise levels to increase in the mid and high frequencies. The noise increase was sufficiently broadband that the jet noise shielding benefits were noticeably reduced.

INTRODUCTION

In order to help meet acceptable community noise standards for future short takeoff and landing (STOL) aircraft, the engine exhaust nozzles can be placed over the wing (OTW) as shown schematically in Fig. 1. With such a configuration, the ground observer is shielded by the wing from some of the engine jet noise radiated to the ground.

In a STOL-OTW configuration the jet flow is required to attach to the wing and flap surfaces. The interaction of the jet flow with the shielding surface causes low frequency noise in excess of that normally associated with nozzle-only jet mixing noise (Ref. 1). This low frequency jet-surface interaction noise also occurs when the jet flow is only partially attached to or even completely detached from the surface, as was shown in Ref. 2. The interaction noise is caused by trailing edge noise due to jet flow interaction with the trailing edge region and jet flow scrubbing noise (also called fluctuating lift noise). A typical STOL OTW configuration noise spectrum is shown in Fig. 2. Current beliefs, not completely substantiated by theory and experiment, are that the noise in the very low frequency region (400 Hz range) is caused

by the fluctuating lift noise source (noise source 1), while that in the mid-frequency range (1250 Hz range) is caused by trailing edge noise (noise source II). In the high frequency range, the shielding surface attenuates the jet noise by the principle of barrier shielding; the amount of shielding depends on a variety of factors including surface length, nozzle configuration, and nozzle size (Refs. 1 to 4).

In Ref. 1, the jet-surface interaction noise sources and jet noise shielding benefits were empirically related to the geometry of the configurations (shielding surface length, nozzle size, nozzle height above the shielding surface, etc.). In the present work, an effort is made to relate the changes in noise level and frequency caused by changes in STOL-OTW configuration geometry to the flow field characteristics normal to the surface at the trailing edge of the shielding surface. This study is aimed principally at the cases of attached and partially attached flow to the shielding surface, although the case of unattached flow will also be considered.

The study, conducted at the NASA Lewis Research Center, was made with a model scale, 5:1 ratio slot nozzle (2.03 cm height and 10.2 cm width) and a simple flat plate that simulated an airfoil. The shielding length of the plate (measured from the nozzle exhaust plane) was varied from 15 to 54.4 cm and the plate had a span of 61 cm. The nozzle exhaust flow was normally parallel to the surface, with the nozzle height from the surface being varied from 0 to 4.45 cm. For a nozzle height of 0.95 cm from the surface, the nozzle also was canted toward the surface by up to 10°.

Mach number contour maps at the trailing edge location were obtained for all nozzle-surface configurations as well as the nozzle only. From these, the Mach number (velocity) profiles at the nozzle centerline were obtained at the trailing edge. Acoustic data were taken only at 90° to the surface, since previous studies had shown little variation of STOL-OTW configuration overall sound pressure levels with directivity angle (Refs. 1 and 2). A jet velocity of 203 m/sec was used to obtain all test data (the effect of jet velocity on STOL-OTW configurations acoustics is given in Refs. 1 and 2).

APPARATUS AND PROCEDURE

Facility

The noise tests were conducted out-of-doors within the 7·15 m courtyard of a subsonic wind tunnel at the Lewis Research Center. A schematic sketch of this facility is shown in Fig. 3. Pressurized air at about 292 K was supplied to a 15.2 cm diameter plenum by twin diametrically opposed supply lines. Airflow through the overhead supply line was measured with a calibrated orifice. The nozzle inlet total pressure was measured with a single probe near the plenum exit flange. Perforated plates and a muffler were located in each system to remove valve noise.

In addition, a bundle of tubes was placed in the plenum to straighten the air flow before it reached the entrance to the nozzle. These devices were located well upstream of the nozzle. Open-cell foam pads were placed on the ground and walls to minimize ground reflections.

Sound pressure level (SPL) spectra were obtained using a 1.27-cm diameter condenser microphone with wind screen. Data were recorded at 90° to the jet axis at a 3.05 meter radius. The noise data were recorded on an FM tape recorder and digitized by a four-second time averaged one-third octave band spectrum analyzer. The analyzer determined sound pressure level spectra in decibels referenced to 2×10^{-5} N/m^2.

Jet Mach number (velocity) profiles were obtained at the downstream trailing edge of the shielding surfaces. Measurements were made with a traversing pitot static tube. The pressures measured were transmitted to an x-y-y' plotter which yielded direct traces on graph paper of the total and static pressure distribution across the jet (Ref. 2).

Acoustic and aerodynamic data were taken at a nominal jet velocity of 203 m/sec (M_j = 0.6).

Models

The test nozzle consisted of a 5:1 slot nozzle with an equivalent diameter of 5.1 cm (Fig. 4(a)).

The jet noise shielding surfaces consisted of simple, flat boards (0.95-cm thick plywood) of 61-cm span and surface lengths downstream of the exhaust nozzle of 15.0, 26.4, and 54.4-cm (Fig. 4(b)). The shielding surface length upstream of the nozzle exhaust plane was 0.6 cm. (In Ref. 2, it was shown that airfoils with flaps retracted and simple boards produce substantially the same acoustic signature.)

Most of the data were taken with the nozzle jet flow directed parallel to the flat plate shielding surface. The nozzle height above the surface was varied from 0 to 4.45 cm. Some data were also taken with the nozzle canted at 5° and a 10° toward the surface with a nozzle height, h, of 0.95 cm. A summary of the geometric variations is tabulated in Fig. 4(b).

AERODYNAMIC DATA

The flow contours, in terms of constant Mach number lines, normal to the surface and in a spanwise plane at the trailing edge are shown in Figs. 5 to 8. The data shown are for nominal nozzle heights, h, of 0, 0.95, and 4.45 cm above the surface and shielding surface lengths of 15.0, 26.4, and 54.4 cm (see Fig. 4).

Effect of nozzle height. - The effect of increasing the nozzle

height from the shielding surface is shown in Figs. 5 to 7 for shielding surface lengths of 15, 26.4, and 54.4 cm, respectively. Also shown in these figures is the effect of canting the nozzle 10° toward the surface with a nozzle height of 0.95 cm. With the shortest surface length (Fig. 5), the Mach number contours were substantially oval in shape for all nozzle heights above the surface. In general, the thickness of the jet flow normal to the trailing edge increased somewhat with increasing nozzle height. With a larger shielding surface length of 26.4 cm, the shape of the flow field became more D-shaped than oval when the nozzle was on or close to the surface (Fig. 6). With a nozzle height of 4.45 cm from the surface, the flow field was still oval. Finally, with the longest shielding surface length of 54.4 cm, the flow field approached a semicircular shape when the nozzle was on or close to the surface (Fig. 7). With a nozzle height of 4.45 cm, the flow field for this surface length was substantially circular in shape (Fig. 7(b)).

Comparisons of the Mach number contour plots shown in Figs. 5 to 7 indicate that with decreasing nozzle height, particularly with shielding surface lengths of 26.4 and 54.4 cm, the peak Mach number increases. For example, in Fig. 6, the peak Mach number for a nozzle height of 4.45 cm is 0.53 (Fig. 6(b)), whereas with the nozzle flush on the surface the peak Mach number is about 0.6 (Fig. 6(a)).

Effect of nozzle canting. - In the (d) portions of Figs. 5 to 7 the effect of canting the nozzle 10° toward the surface on the Mach number contour plots is shown side by side with the parallel flow plots ((c) portions of figures). Both sets of contours were obtained for a nozzle height above the shielding surface of 0.95 cm. It is apparent that canting the nozzle spreads the jet flow spanwise along the trailing edge to a much greater extent than that with the nozzle parallel to the surface for all surface lengths. Furthermore, the height of a given Mach number contour line above the surface is decreased when the nozzle is canted compared to a parallel nozzle orientation to the surface. However, it is also apparent that the canting of the nozzle by 10° had only a small effect on the peak Mach number at the trailing edge for each shielding surface length.

Effect of shielding surface length. - The Mach number contours obtained with the nozzle flush to the shielding surface at the various surface lengths are taken from Figs. 5(a), 6(a), and 7(a) and reassembled in Fig. 8 to illustrate the typical effect of shielding surface length on the flow field at the trailing edge of the plate. The change in shape of the contour map from an oval shape to a D-shape is apparent. Also, the increase in the profile height for constant Mach number contours, as well as some increase in overall width of the jet flow is clearly evident. The peak Mach number is seen to decrease with increasing shielding surface length, from 0.6 with a surface length of 15 cm to 0.5 with a surface length of 54.4 cm. Similar trends were observed at other nozzle heights.

Mach number centerline profiles. - The variation of local Mach number at the trailing edge as a function of height above the surface (nor-

5

mal to the chord) at the nozzle centerline for several nozzle locations above the surface and fixed surface lengths is shown in Fig. 9. The changes in the profiles including the peak Mach number discussed previously are clearly evident in these plots. Also noted in Fig. 9 is the peak Mach number of the nozzle only at the various surface trailing edge locations. Except for the case of the shortest shielding surface (15.0 cm), the effect of decreasing the nozzle height from the surface is to increase the peak Mach number, as previously noted. For the shortest surface, the surface length was not enough to alter the jet flow sufficiently to affect the Mach number decay characteristics of the nozzle flow. The data show that the peak Mach number, in general, decreases with increases in both surface length and nozzle height.

ACOUSTIC DATA

The acoustic data herein were obtained at a directivity angle of 90° and are presented in terms of SPL as a function of frequency. The pertinent data are given in Figs. 10 to 13 and the data trends are summarized briefly in the following sections.

Nozzle Only

For reference and comparison purposes, the spectrum for the nozzle only is given in Fig. 10. The curve shown in the figure is faired through the data and will be used in subsequent comparisons with the nozzle-surface acoustic data.

Nozzle with Shielding Surface

Effect of nozzle height. - The effect of nozzle height from the shielding surface on the spectra is shown in Fig. 11. Also shown, for comparison, is the nozzle-only spectrum. With increasing nozzle height the SPL values in the frequency range of 800 to 2000 Hz generally are reduced. The SPL values in the lower frequency range (200 to 500 Hz) generally increase with an increase in nozzle height from the shielding surface. In addition, the shielding benefits, in terms of the difference between the SPL's for the nozzle-wing and nozzle only (ΔSPL), generally are increased with increasing nozzle height above the shielding surface.

Effect of shielding surface length - The effect of surface length at several nozzle heights above the surface is shown also by the data in Fig. 11 and illustrated for clarity in Fig. 12 for the case of the nozzle flush to the surface. With increasing surface length the peak SPL values occur at decreasing frequencies. A second SPL peak occurs in the 200 to 500 Hz frequency range with the 54.4 cm long shielding surface. When the nozzle is flush with the shielding surface, the peak SPL value of the spectra decreases with increasing surface length. With a nozzle

height of 0.95 cm, the peak SPL of the spectra remains substantially con-
stant, although the frequency at which the peak SPL occurs shifts to
lower frequencies with increasing surface length.

In general, increased shielding benefits (greater ΔSPL values at a
given frequency) were obtained at the higher frequencies with increases
in the shielding surface length.

Effect of nozzle cant angle. - With increasing nozzle cant angle,
the SPL near the peak SPL values generally increase as shown in Fig. 13.
The increase in peak SPL with nozzle cant angle amounts to about 3 dB for
the shortest surface length (15 cm) and decreases with increasing surface
length. Furthermore, an increase in SPL with increasing nozzle cant angle
occurs at the higher frequencies resulting in lower ΔSPL values, thus re-
ducing the shielding benefits compared with the case of parallel flow.
At the same time, a decrease in SPL occurs at the lower frequencies.
These trends are also evident with a shielding surface length of 26.4 cm
and to lesser extent with the longest surface length of 54.4 cm.

CORRELATION OF ACOUSTIC DATA WITH AERODYNAMIC DATA

Analysis

The low and mid-frequency noise increase observed with OTW configu-
rations (Figs. 11 to 13) compared with the noise level of the nozzle only
spectra is caused by two primary noise sources. The spectra ascribed to
these noise sources are shown schematically in Fig. 14(a) in terms of SPL
as a function of frequency. The low frequency noise (noise source I in
Fig. 14(a)) is currently believed to be associated with the fluctuating
lift noise on the surface, while the mid-frequency noise (noise source II
in Fig. 14(a)) is currently believed to be caused by trailing edge noise
associated with the jet flow interaction with the shielding surface trail-
ing edge. These interpretations supercede the source identifications
speculated in Ref. 2. In Ref. 2, different spectral shapes, based on
curves faired through the data, were proposed for these two noise sources
based on unattached and partially attached flow cases associated with cir-
cular nozzles and shielding surfaces. For the present study with the 5:1
slot nozzle representative spectral shapes are taken as shown in Fig. 14(b).
These representative spectra differ slightly from those of Ref. 2, partic-
ularly the spectrum for noise source II which has a steeper ascending
slope than that of Ref. 2.

Furthermore, in the region of jet noise shielding, the data indicate
the apparent presence of a high frequency jet-surface interaction noise
source that peaks at about 6300 Hz (Fig. 11). This noise source could
also be related to fluctuating lift or body forces as discussed in Ref. 5.
Refraction effects at the trailing edge could also be contributing to the
establishment of a noise floor. The data, herein, are insufficient to
permit an evaluation of this possible additional jet-surface interaction
noise source.

In attempting to analyze the acoustic data trends for attached and partially attached flow in terms of the jet flow characteristics measured at the trailing edges of the shielding surfaces, the flow related variables shown schematically in Fig. 15 appear to be most important. The δ_T term represents the jet boundary layer height at the trailing edge and is specified by the maximum velocity, U_m, of the velocity profile (Mach number profile) at the trailing edge of the shielding surface. The δ_e term defines the effective height of the jet free-shear boundary. This height is determined by the point at which the local flow velocity in the free shear layer of the jet is $0.8\ U_m$. Velocities less than this value of $0.8\ U_m$ are considered not to contribute significantly to the overall noise level.

With unattached flow the term δ_F is determined at the thickness of the outer jet shear flow boundary at the point where the local velocity is 0.8 of the maximum local boundary velocity, $U_{F,m}$, when the jet flow is completely detached from the surface at the trailing edge. With the present 5:1 slot nozzle, the value of δ_S was obtained by a straight-line projection along the Mach number (velocity) profile to an intersection with the ordinate (zero Mach number). Because the flow field velocity contours are substantially unchanged in shape, when referenced to the jet velocity (the absolute level of velocity, of course, does change with U_j), this procedure is assumed to be valid for a wide range of subsonic jet velocities.

Noise source I. - On the basis of the acoustic and aerodynamic data, the following equations were developed empirically to describe noise source I. The peak sound pressure level, $SPL_{p,I}$, is calculated by:

$$SPL_{p,I} = 97.5 - 10 \log U_m + 20 \log \delta_e \tag{1}$$

or, in terms of nozzle height, H, and jet velocity, U_j,

$$SPL_{p,I} = 80.5 + 20 \log\left(\frac{\delta_e}{H}\right) + 10 \log\left(\frac{U_j}{U_m}\right) \tag{2}$$

The terms H and U_j in Eq. (2) are introduced to provide dimensionless parameters for the present work. However, it should be noted that δ_e and U_m are directly dependent on a characteristic geometry dimension such as H and a velocity such as U_j, respectively. Furthermore, although not included in the present scope of the work, it is shown in Ref. 2 that $SPL_{p,I}$ is also a function of U_j^3, nozzle size, etc. Because these terms are constants herein, they are included as part of the constant in Eq. (1). In summary, the peak SPL of noise source I is a primary function of the effective jet free shear boundary thickness at the trailing edge and the peak velocity of the jet flow at the trailing edge.

The frequency at which $SPL_{p,I}$ occurs was determined as:

$$f_{p,I} = 0.22\left(\frac{U_j}{L}\right)(L/H)^{0.33} \tag{3}$$

Noise source II. - The evaluation of suitable parameters for correlating noise source II resulted in the following equations. The peak SPL value was determined by:

$$SPL_{p,II} = 25 - 10 \log \delta_e + 30 \log U_m \tag{4}$$

or, in terms of nozzle height, H, and jet velocity, U_j,

$$SPL_{p,II} = 94.2 - 10 \log\left(\frac{\delta_e}{H}\right) - 30 \log\left(\frac{U_j}{U_m}\right) \tag{5}$$

The terms H and U_j were again used to provide nondimensional terms. Furthermore, according to Ref. 2, the peak SPL for noise source II should also be a function of U_j^0, nozzle size, etc. As noted previously, these variables were not included herein, and thus constitute part of the constant in Eq. (4).

Reasonable correlation of the data can be obtained also by the use of δ_T; however, the agreement between measured and calculated SPL values is not as good as when δ_e is used. The equations when δ_T is used are as follows:

$$SPL_{p,II} = 22 - 10 \log \delta_T + 30 \log U_m \tag{6}$$

The frequency at which $SPL_{p,II}$ occurs is given by

$$f_{p,II} = 0.5\left(\frac{U_j}{L}\right)(L/H)^{0.33} \tag{7}$$

With the nozzle located 4.45 cm above the shielding surface, the trailing edge velocity surveys had indicated jet flow detachment with the 15 and 26.4 cm shielding surface lengths. (Jet flow attachment is still indicated for the 54.4 cm length.) The detachment of the jet flow from the surface causes the level of the interaction noise source I to become less than that with a nozzle height above the surface of 1.9 cm. As a consequence, all the equations developed herein for predicting the noise source levels do not apply to cases where flow detachment has occurred or is imminent.

Comparison of Measured and Calculated Spectra

The measured SPL values of noise sources I and II are compared in Figs. 16 to 19 with calculated spectra based on Eqs. (1) to (5) and (7)

and the spectral shapes given in Fig. 14(b). The solid points in Figs. 16 to 19 represent the antilogarithmic subtraction of the nozzle-only SPL values from the nozzle-surface SPL values when these noise sources coincide. In general, good agreement in spectral distribution between the measured data and that based on the empirically developed model is evident for the entire range of variables included in this study. In particular, it is apparent that the equations account well for variations in shielding length, nozzle height above the surface (partially attached flow) and canting the nozzle toward the shielding surface to promote improved flow attachment to the surface.

Jet Noise Correlation in Shielding Region

The data shown in Fig. 11 indicate that with increasing nozzle height above the shielding surface, the amount of jet noise shielding at high frequencies provided by the surface increases; consequently, the SPL values are reduced compared with those for the nozzle only. It was also demonstrated in Ref. 2 that when the jet flow is substantially detached from the surface, no additional shielding benefits are obtained with further increases in nozzle height from the shielding surface. The increase in ΔSPL with an increase in nozzle height is correlated herein by the shielding parameter, ψ, given by

$$\psi = \left(\frac{fL}{U_{F,m}} \right) \left(\frac{\delta_e}{\delta_F - \delta_s} \right) \tag{8}$$

where $\delta_F - \delta_s$ and $U_{F,m}$ are reference values (see Fig. 15).

The correlation of the SPL for the high frequency jet noise shielding region is shown in Fig. 20 in terms of Eq. (8). The data are shown separated by shielding surface length for clarity; the solid curves shown faired through the data in the figure parts provide the same reference for the data. It is apparent that excellent agreement of the acoustic data has been achieved for all three surface lengths and nozzle geometry variations.

In Fig. 21, an example of the variation of SPL and ΔSPL with the degree of jet flow attachment to the shielding surface is illustrated. The curves shown in the figure are based on the aerodynamic and acoustic data contained herein. For the example, a shielding surface length of 26.4 cm was selected. The nozzle-only curve shown for comparison purposes in Fig. 21(a) was taken from Fig. 10.

The maximum shielding benefits, according to Eq. (8) are obtained when the jet flow is completely detached from the shielding surface; i.e., $\delta_e/(\delta_F - \delta_s) = 1.0$. This case is shown in Fig. 21 by the dashed curves. (It should be noted that the shape of the ΔSPL curve in Fig. 21(b) is the same as that given in Ref. 2.) The minimum shielding benefits are obtained when the jet flow is firmly attached to the shield-

ing surface. This case is shown by the dash-double dot curves in Fig. 21 which represent a nozzle mounted flush to the shielding surface and with the jet flow parallel to it. Similar results were obtained with the nozzle mounted 0.95 cm above the surface but canted 10° toward it. With increasing nozzle height above the surface and parallel jet flow to it $(\delta_e/(\delta_F - \delta_s) < 1.0)$, the shielding benefits are increased, in terms of lower SPL and higher ΔSPL values.

These latter cases represent partial jet flow attachment to the shielding surface, with less attachment being associated with greater nozzle heights above the shielding surface. Results similar to those shown in Fig. 21 also occur with the shielding surface lengths of 15.0 and 54.4 cm used in this study.

CONCLUDING REMARKS

On the basis of the present study, it has been shown that the acoustics of simple STOL-type OTW configurations with a 5:1 slot nozzle can be related to the aerodynamic characteristics at the trailing edge of the shielding surface. However, the limited scope of the present work, with respect to nozzle size and shape, surface curvature effects, etc., indicate additional work needs to be done to provide more complete acoustic and aerodynamic parameters. For example, in Ref. 2, a nozzle size parameter was required to provide correlation for the OTW configuration shielding data with circular nozzles. A brief comparison of these data with the present work indicates that the parameter needs to be modified to include a term that reflects the aspect ratio of a noncircular nozzle. The present work indicates that inclusion of the square root of the aspect ratio may provide correlation; however, this must be verified through tests with slot nozzles having aspect ratios other than 5:1.

The effect of greater jet flow impingement angles (nozzle cant angle) on the spectral content of OTW configurations must also be further evaluated. The present data indicate that the noise level can be increased with a change from parallel jet flow to the surface to one impinging at only 10° to the surface. The use of large jet flow impingement angles to the surface stems from the aerodynamic need to maintain flow attachment to deflected flap or curved wing surfaces. Impingement of the nozzle flow on the surfaces with an internal (nozzle roof or kick-down angle) or an external deflector promotes such jet flow attachment. Unfortunately, the use of the 10° canted nozzle also reduced the amount of jet noise shielding provided by the shielding surface.

NOMENCLATURE
(All symbols are in S.I. units unless noted.)

f   frequency

H   nozzle height

h   nozzle height above shielding surface

L   shielding surface length downstream of nozzle exhaust plane

M   Mach number

SPL   sound pressure level of nozzle-surface configuration, dB re 2×10^{-5} N/m^2

SPL_N sound pressure level of nozzle only, dB re 2×10^{-5} N/m^2

ΔSPL $SPL - SPL_N$, dB

U   velocity

δ jet boundary characteristic dimension

ψ shielding parameter, $(fL/U_{F,m})(\delta_e/(\delta_F - \delta_s))$

I, II   jet-surface interaction noise source identification

Subscripts:

e   effective jet free shear boundary

F   jet free shear boundary height with detached flow

j   jet

m   maximum

p   peak

s   lower jet free shear boundary height from shielding surface

T   trailing edge of shielding surface

REFERENCES

1. M. Reshotko, J. H. Goodykoontz, and R. G. Dorsch, "Engine-Over-the-Wing Noise Research," AIAA paper 73-631, pp. 1-15 (1973).

2. U. von Glahn, D. Groesbeck, and M. Reshotko, "Geometry Considerations for Jet Noise Shielding with CTOL Engine-Over-the-Wing Concept," AIAA paper 74-568, pp. 1-40 (1974).

3. U. von Glahn, and D. Groesbeck, "Influence of Mixer Nozzle Velocity Decay Characteristics on CTOL-OTW Jet Noise Shielding," AIAA paper 75-97, pp. 1-13 (1975).

4. U. von Glahn, and D. Groesbeck, "Influence of Multitube Mixer Nozzle
   Geometry on CTOL-OTW Jet Noise Shielding," NASA TM X-71681,
   pp. 1-21 (1975).

5. R. E. Hayden, "Fundamental Aspects of Noise Reduction from Powered-
   Lift Devices," SAE paper 730376, pp. 1-43 (1973).
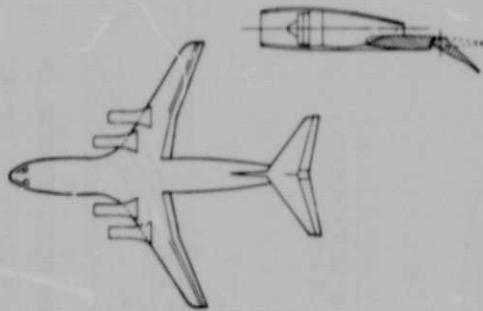
Figure 1. - Engine over-the-wing concept for STOL aircraft.
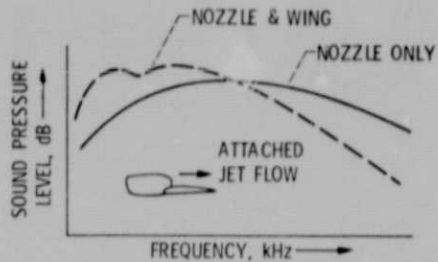

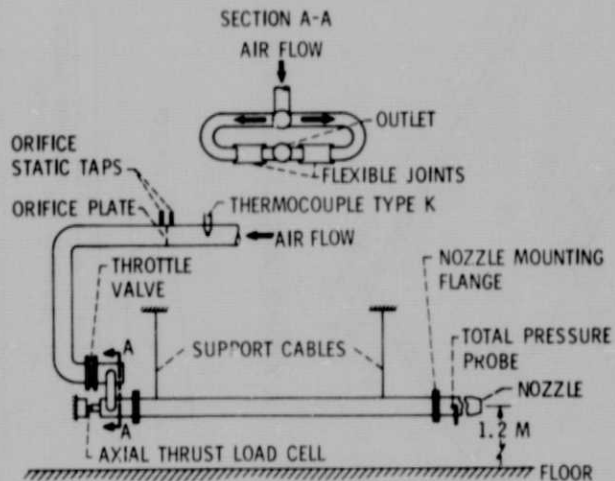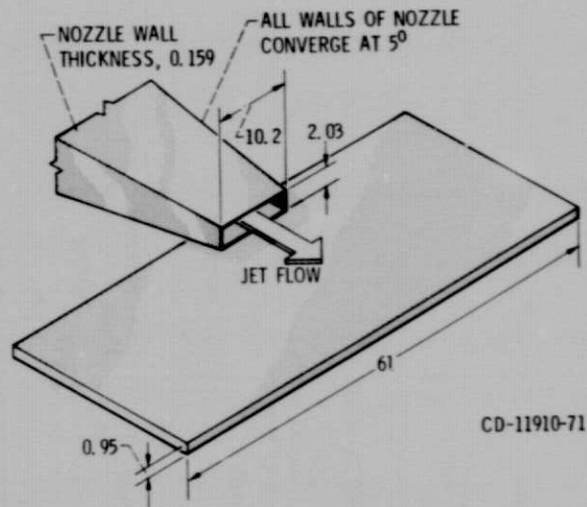Figure 2. - Schematic of STOL-OTW noise spectrum compared with nozzle only spectrum.

Figure 3. - Schematic diagram of courtyard test rig.

NOZZLE WALL THICKNESS, 0.159

ALL WALLS OF NOZZLE CONVERGE AT 5°

10.2 2.03

JET FLOW

61

0.95

CD-11910-71

(a) SCHEMATIC SKETCH OF NOZZLE AND FLAT PLATE.

H = 2.03

h

SHIELDING SURFACE LENGTH, L

6.6
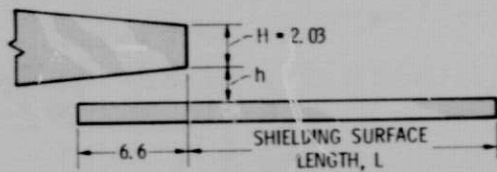
| NOZZLE HEIGHT ABOVE SURFACE, h | 0, 0.95, 1.9, 3.2, 4.45 |
| SURFACE LENGTH, L | 15.0, 26.4, 54.4 |

(b) NOZZLE-TO-SHIELDING SURFACE ORIENTATION.

Figure 4. - Schematic sketch of nozzle-shielding surface configurations. All dimensions in centimeters.

LOCAL MACH NO.

(a) NOZZLE HEIGHT, FLUSH.

(b) NOZZLE HEIGHT, 4.4 CM.

(c) NOZZLE HEIGHT, 0.95 CM.

(d) NOZZLE HEIGHT, 0.95 CM; NOZZLE CANTED 10°.

HEIGHT NORMAL TO TRAILING EDGE, CM

SPANWISE DISTANCE MEASURED FROM NOZZLE CENTERLINE, CM
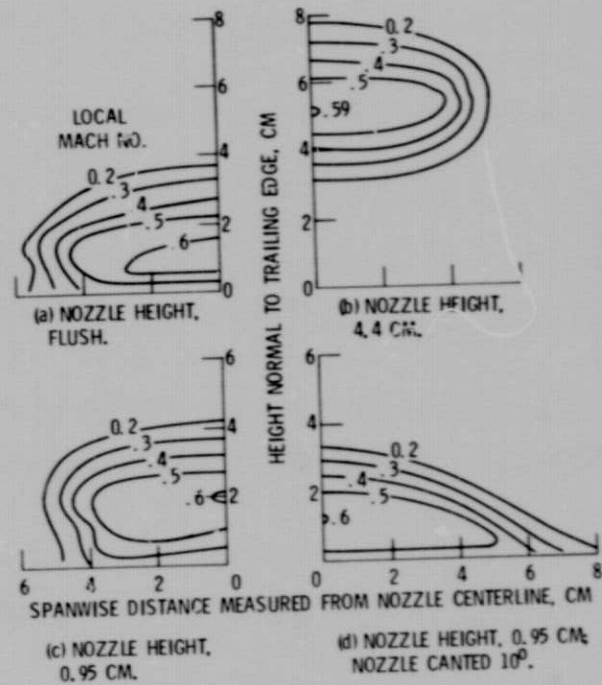
Figure 5. - Mach number contour maps at trailing edge of shielding surface with surface length of 15.0 cm. M_j, 0.6.
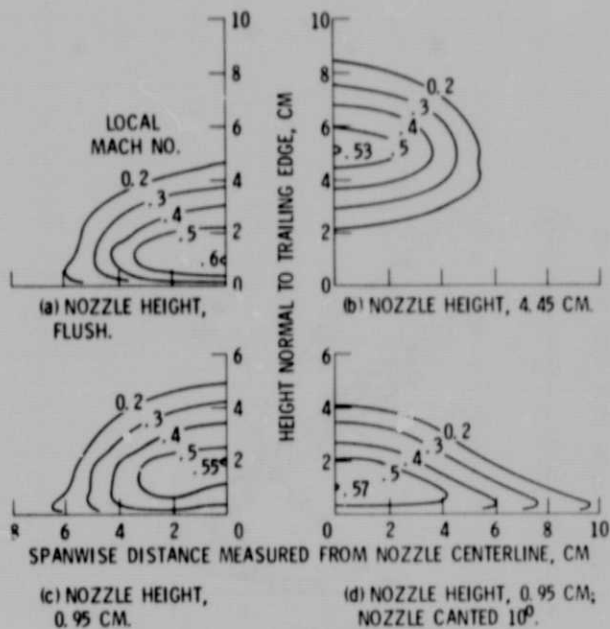
Figure 6. - Mach number contour maps at trailing edge of shielding surface with surface length of 26.4 cm. M_j, 0.6.
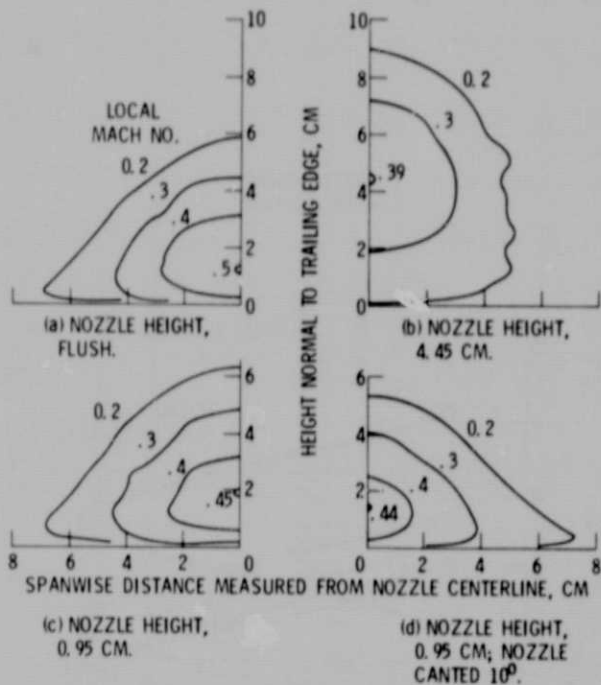

Figure 7. - Mach number contour maps at trailing edge of shielding surface with surface length of 54.4 cm. M_j, 0.6.
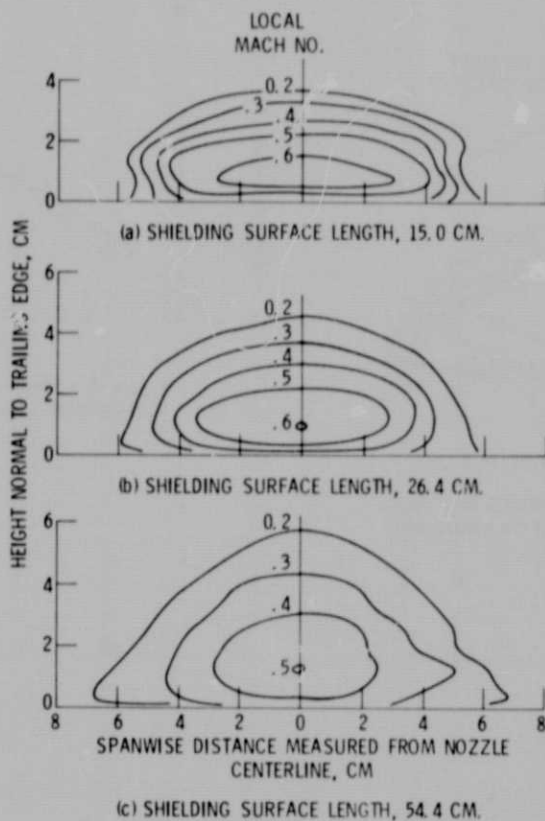

Figure 8. - Variation of Mach number contour maps at trailing edge of shielding surface for several surface lengths. Nozzle flush to shielding surface; M_j, 0.6.
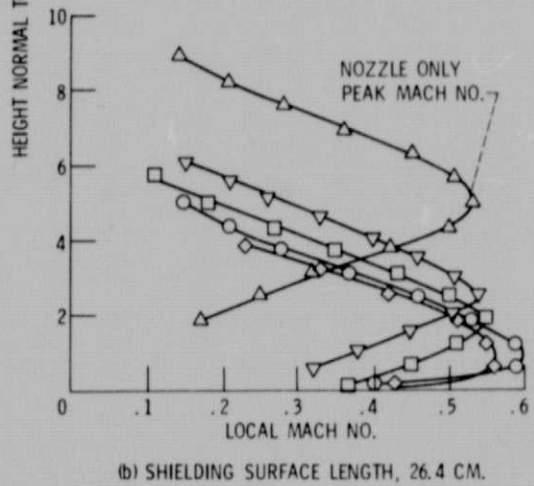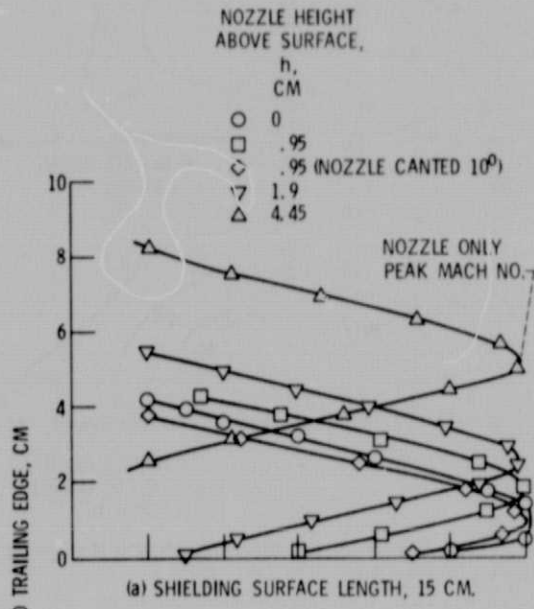
NOZZLE HEIGHT
ABOVE SURFACE,
h,
CM
○ 0
□ .95
◇ .95 (NOZZLE CANTED 10°)
▽ 1.9
△ 4.45

NOZZLE ONLY
PEAK MACH NO.

(a) SHIELDING SURFACE LENGTH, 15 CM.

HEIGHT NORMAL TO TRAILING EDGE, CM

LOCAL MACH NO.

NOZZLE ONLY
PEAK MACH NO.

(b) SHIELDING SURFACE LENGTH, 26.4 CM.

Figure 9. - Velocity profiles, in terms of local Mach number, on nozzle centerline at the trailing edge of the shielding surface. M_j, 0.6.
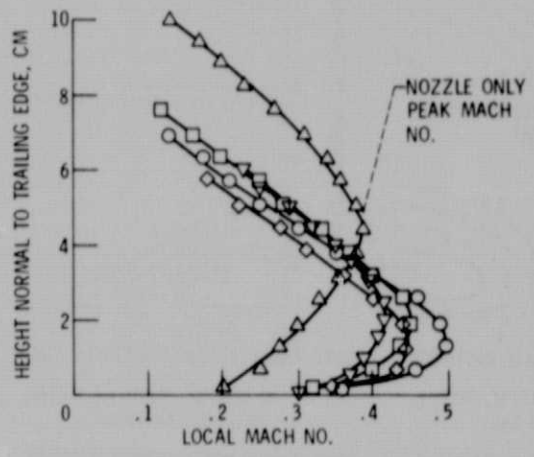
NOZZLE ONLY
PEAK MACH
NO.

(c) SHIELDING SURFACE LENGTH, 54.4 CM.

Figure 9. - Concluded.
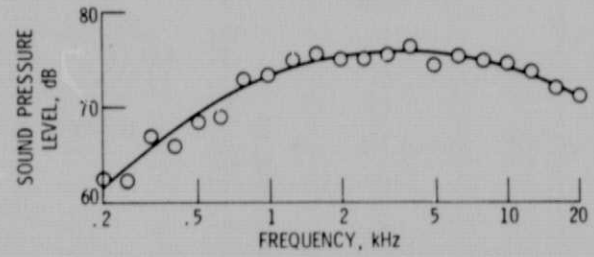
SOUND PRESSURE LEVEL, dB

FREQUENCY, kHz

Figure 10. - Nozzle-only one-third octave band sound pressure level spectrum. M_j, 0.6.
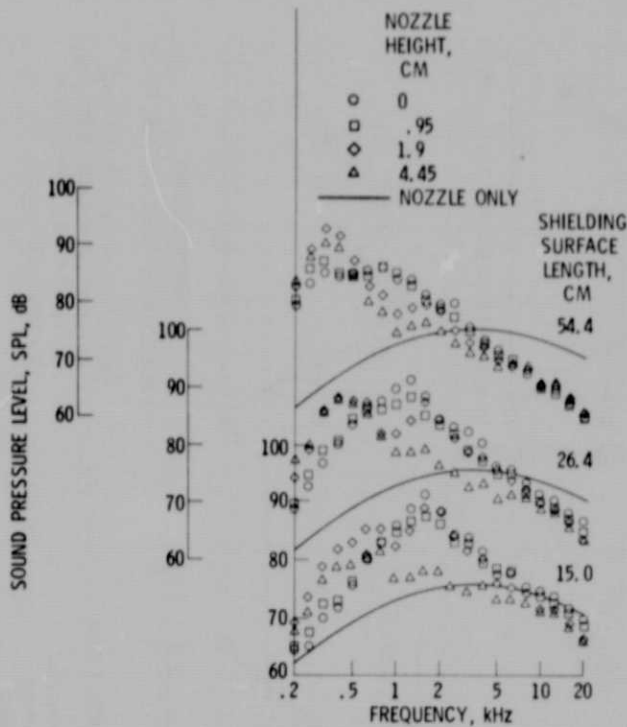
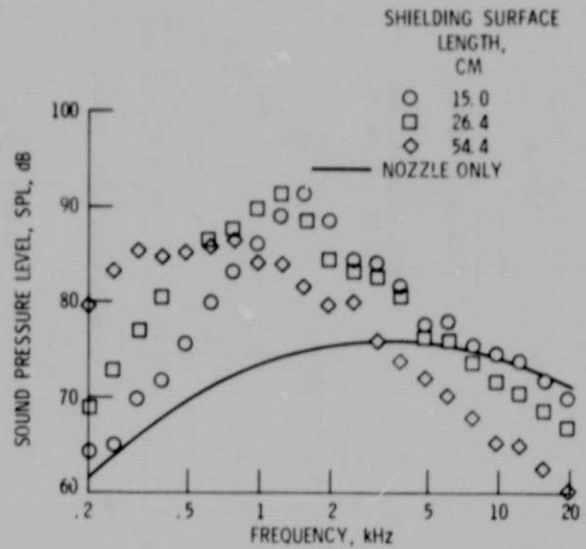Figure 11. - Effect of nozzle height above shielding surface on sound pressure levels. M_j, 0.6.

Figure 12. - Representative effect of shielding surface length on sound pressure levels. Nozzle flush on shielding surface. M_j, 0.6.
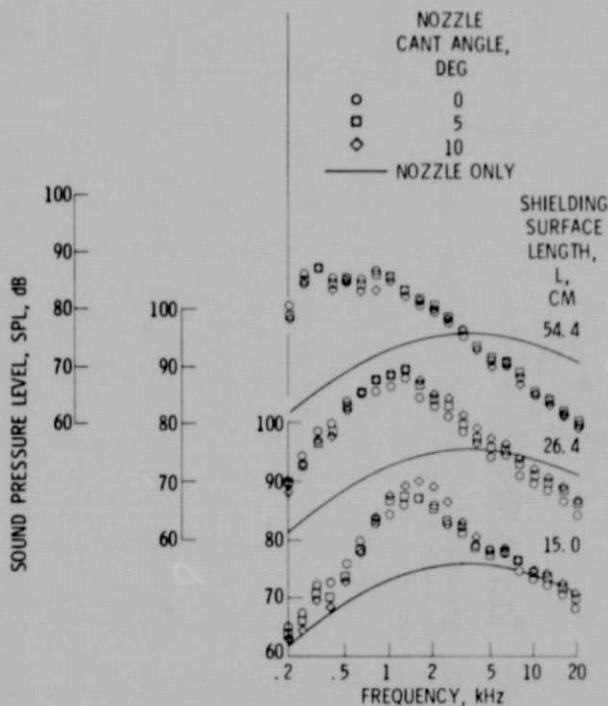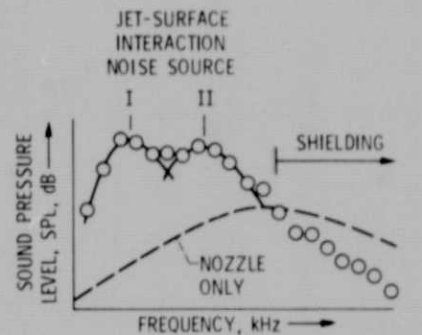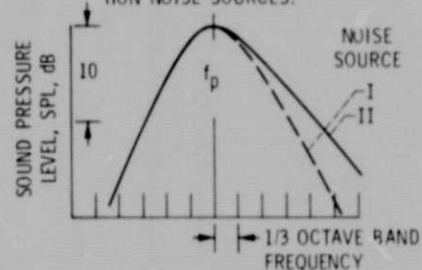

Figure 13. - Effect of nozzle cant angle on sound pressure levels. Nozzle height above surface, 0.95 cm; M_j, 0.6.

(a) INDENTIFICATION OF LOW FRE-QUENCY JET-SURFACE INTERAC-TION NOISE SOURCES.

(b) REPRESENTATIVE JET-SURFACE IN-TERACTION NOISE SPECTRAL DIS-TRIBUTIONS.

Figure 14. - Jet-surface interaction noise sources and spectral characteristics.
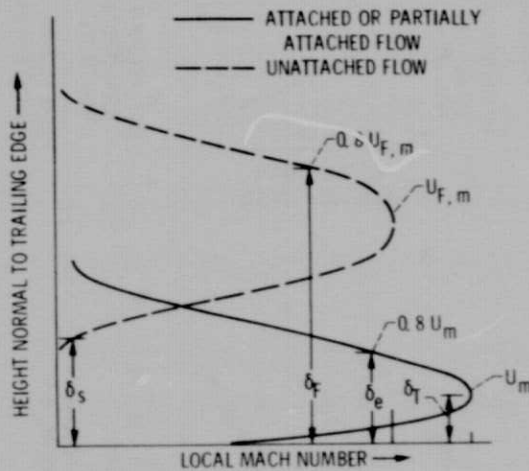
Figure 15. - Schematic sketch of jet boundary flow characteristic dimensions at trailing edge of shielding surface.

(a) NOZZLE HEIGHT ABOVE SURFACE, 0 CM.

(b) NOZZLE HEIGHT ABOVE SURFACE, 0.95 CM.

(c) NOZZLE HEIGHT ABOVE SURFACE, 1.9 CM.

Figure 16. - Comparison of measured and calculated interaction noise source SPL values. Shielding surface length, 15 cm; M_j, 0.6.

CALCULATED NOISE SOURCE
—— I
—— - II
O MEASURED VALUES
SOLID SYMBOLS INDI-
CATE CORRECTION FOR
NOZZLE - ONLY NOISE

(a) NOZZLE HEIGHT ABOVE SURFACE, 0 CM.

(b) NOZZLE HEIGHT ABOVE SURFACE, 0.95 CM.

(c) NOZZLE HEIGHT ABOVE SURFACE, 1.9 CM.

Figure 17. - Comparison of measured and calculated interaction noise sour source SPL values. Shielding sur- face length, 26.4 cm; M_j, 0.6.

CALCULATED NOISE
SOURCES

———— I
—·—·— II
O MEASURED VALUES

SOLID SYMBOLS INDI-
CATE CORRECTION FOR
NOZZLE - ONLY NOISE

(a) NOZZLE HEIGHT ABOVE SURFACE,
0 CM.

(b) NOZZLE HEIGHT ABOVE SURFACE,
0. 95 CM.

(c) NOZZLE HEIGHT ABOVE SURFACE,
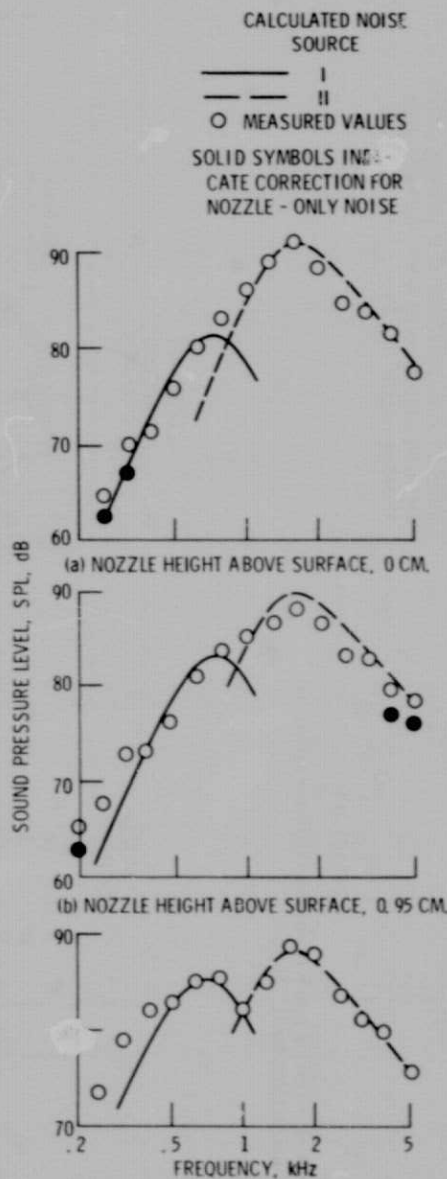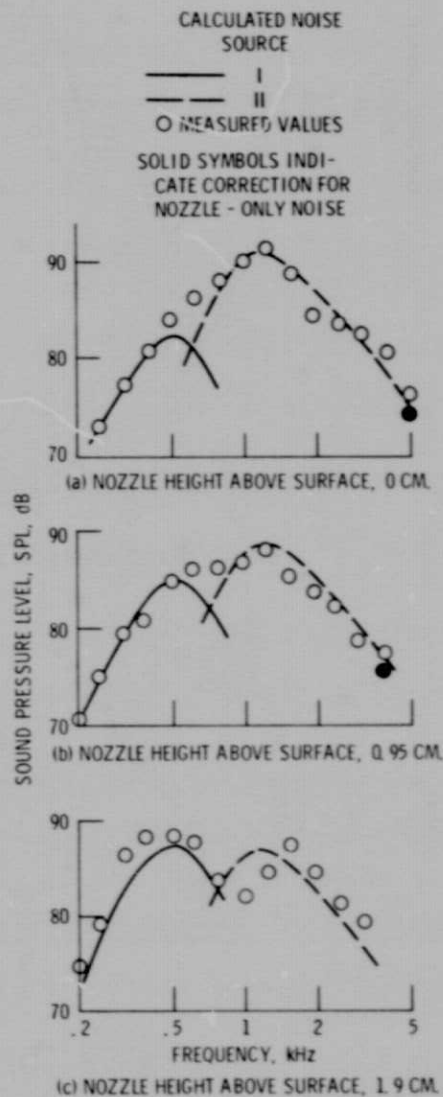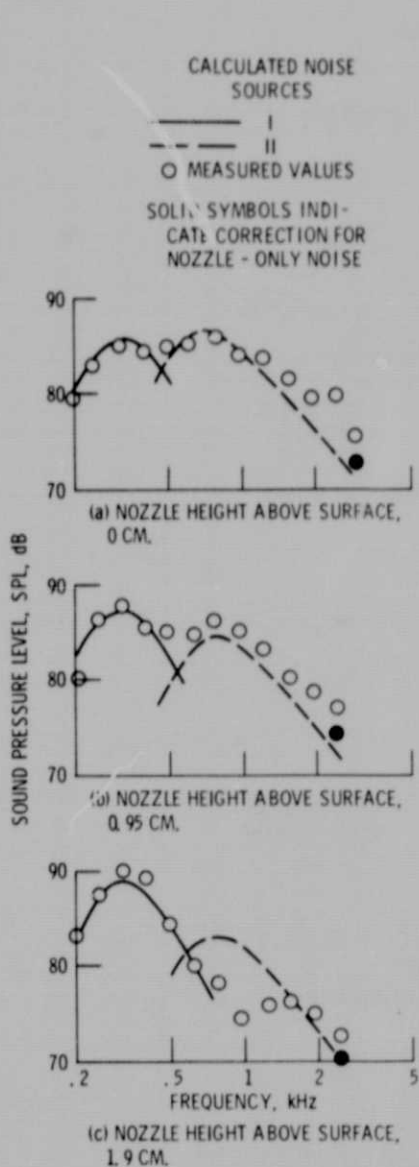1. 9 CM.

SOUND PRESSURE LEVEL, SPL, dB

FREQUENCY, kHz

Figure 18. - Comparison of measured
and calculated interaction noise
source SPL values. Shielding sur-
face length, 54. 4 cm; M_j, 0. 6.

CALCULATED NOISE
SOURCE

———— I
—·—·— II
O MEASURED VALUES

SOLID SYMBOLS INDI-
CATE CORRECTION FOR
NOZZLE - ONLY NOISE

(a) SHIELDING LENGTH, 15 CM.

(b) SHIELDING LENGTH, 26. 4 CM.

(c) SHIELDING LENGTH, 54. 4 CM.

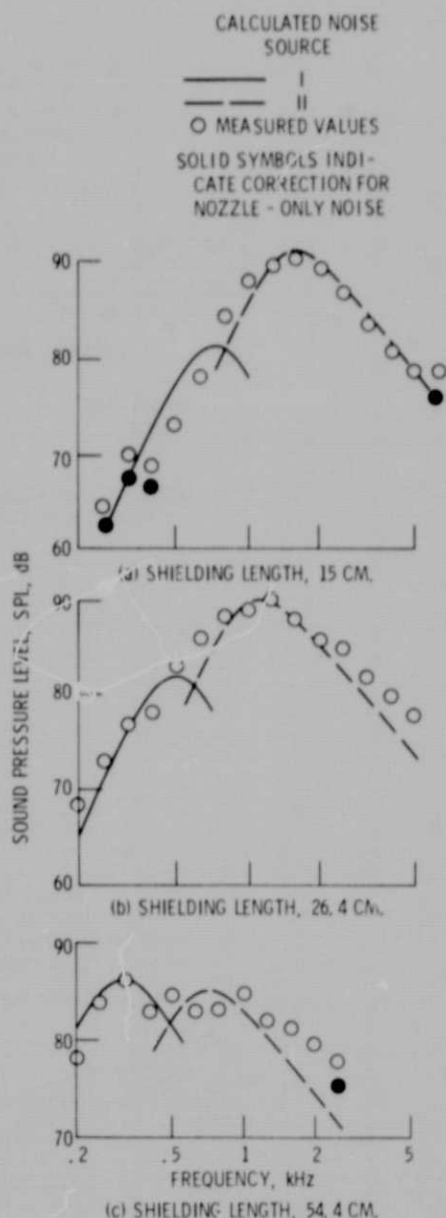SOUND PRESSURE LEVEL, SPL, dB

FREQUENCY, kHz

Figure 19. - Comparison of measured
and calculated interaction noise
source SPL values with nozzle
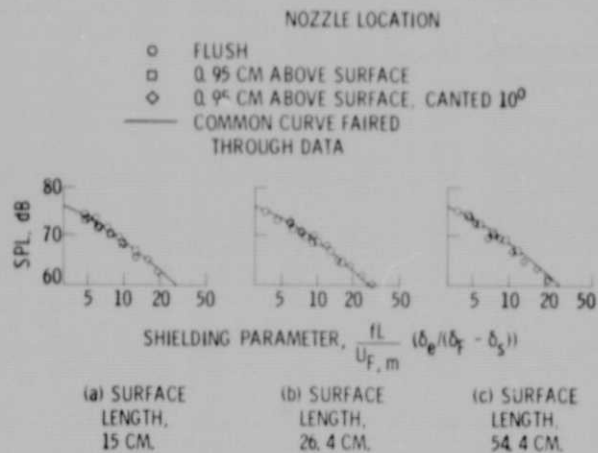canted 10^0. Nozzle height above
surface, 0. 95 cm

NOZZLE LOCATION

○   FLUSH
□   0. 95 CM ABOVE SURFACE
◇   0. 95 CM ABOVE SURFACE, CANTED 10^0
── COMMON CURVE FAIRED
    THROUGH DATA

SPL, dB

SHIELDING PARAMETER, $\frac{fL}{\bar{U}_{F,m}} (\delta_e/(\delta_F - \delta_s))$

(a) SURFACE	(b) SURFACE	(c) SURFACE
LENGTH,	LENGTH,	LENGTH,
15 CM.	26. 4 CM.	54. 4 CM.

Figure 20. - Correlation of SPL in high frequency jet noise shielding region. M_j, 0.6.

JET-SURFACE FLOW CONDITION	NOZZLE HEIGHT ABOVE SURFACE, CM
── NOZZLE ONLY	----
── ○ FLOW DETACHED	4. 45
── □ FLOW PARTIALLY ATTACHED	0. 95
── ◇ FLOW COMPLETELY ATTACHED	0

ALL SHIELDING CURVES SHOWN ARE CALCULATED

SPL, dB

ΔSPL, dB

FREQUENCY, kHz

(a) REDUCTION IN SPL WITH DECREASED JET FLOW ATTACH-MENT.
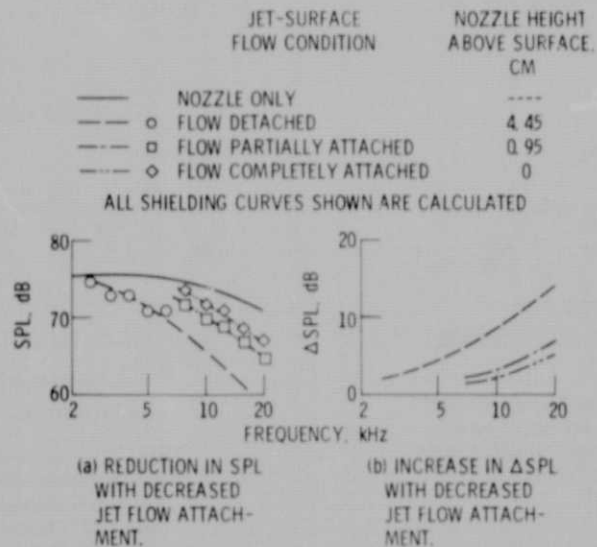
(b) INCREASE IN ΔSPL WITH DECREASED JET FLOW ATTACH-MENT.

Figure 21. - Effect of degree of jet flow attachment to shielding surface on shielding benefits. Shielding surface length, 26. 4 cm; M_j, 0.6.